

Compensatory dynamics of fish recruitment illuminated by functional elasticities

Justin D. Yeakel · Marc Mangel

Received: date / Accepted: date

Abstract Models of Stock Recruitment Relationships (SRRs) are often used to predict fish population dynamics. Commonly used SRRs include the Ricker, Beverton-Holt, and Cushing functional forms, which differ primarily by the degree of density dependent effects (compensation). The degree of compensation determines whether recruitment respectively decreases, saturates, or increases at high levels of spawning stock biomass. In 1982 J.G. Shepherd united these dynamics into a single model, where the degree of compensation is determined by a single parameter, however the difficulty in relating this parameter to biological data has limited its usefulness. Here we use a generalized modeling framework to show that the degree of compensation can be related directly to the functional elasticity of growth, which is a general quantity that measures the change in recruitment relative to a change in biomass, irrespective of the specific SRR. We show that the elasticity of growth can be calculated from short-term fluctuations in fish biomass, is robust to observation error, and can be used to determine general attributes of the SRR in both continuous time production models, as well as discrete time age-structured models. This framework may be particularly useful if fisheries time-series data are limited, and not conducive to determining functional relationships using traditional methods of statistical best-fit.

J.D. Yeakel
Center for Stock Assessment Research &
Department of Ecology and Evolutionary Biology,
University of California Santa Cruz, Santa Cruz, CA 95064, USA.
E-mail: jdyeakel@gmail.com
Tel:+1.831.706.4215

M. Mangel
Center for Stock Assessment Research &
Department of Applied Mathematics and Statistics,
University of California Santa Cruz, Santa Cruz, CA 95064,
USA and Department of Biology, University of Bergen, Bergen 5020, Norway
E-mail: msmangel@ucsc.edu

Keywords Compensatory dynamics · Generalized modeling · Stock-recruitment relationships · Shepherd function · Neimark-Sacker

1 Introduction

Recruitment plays a central role in the population dynamics of fish species. Models of fish recruitment include both density-independent and -dependent effects, controlled by the variables α and β , respectively. That is, when density-dependent effects are negligible, recruitment is generally modeled as $S(B) = \alpha B$, where $S(B)$ is the level of recruitment when B is spawning stock biomass, and α is the recruitment rate in the absence of density-dependent effects (e.g. Sissenwine and Shepherd 1987). We note that recruitment functions are often introduced as $R(B)$, but to prevent confusion later on (where we introduce scaled functions denoted by lowercase letters, such that r could be confused as a growth rate), we avoid the use of R to denote recruitment. In using spawning biomass, we have followed a relatively standard assumption of fishery science that fecundity is proportional to biomass.

When density-dependent effects are non-negligible, recruitment is anticipated to deviate from this relationship, such that $S(B) = \alpha BF(\beta, B)$, where the function F controls density-dependent effects on recruitment. Traditional stock recruitment models introduce three general kinds of density-dependent responses to increasing spawning stock biomass: 1) recruitment increases to a maximum and then declines as B increases, 2) recruitment saturates as B increases, 3) as B increases, recruitment continues to increase but at a lower rate than in the absence of density-dependent effects. These alternative scenarios thus differ in the intensity of density dependence (degree of compensation), which determines to what extent recruitment is altered as a function of spawning stock biomass.

Ricker (1954) developed a Stock-Recruitment Relationship (SRR) to introduce
 48 declines in recruitment at high levels of spawning stock biomass (Fig. 1a),

$$S(B) = \alpha B e^{-\beta B}. \quad (1)$$

As spawning stock biomass increases, recruitment increases to the maximum $S(B) =$
 50 $1/\beta$ and then declines. The Ricker model is used if there are predatory response lags,
 when greater stock abundance suppresses juvenile growth, or when cannibalism or
 52 nest predation limits recruitment when B is high (Cushing 1988).

Beverton and Holt (1957) introduced a related two parameter model where

$$S(B) = \frac{\alpha B}{1 + \beta B}, \quad (2)$$

54 Recruitment is thus a saturating function of spawning stock biomass, where satura-
 tion occurs at $S(B) = \alpha/\beta$ as $B \rightarrow \infty$. Here, it is assumed that density-dependent
 56 mortality affects recruitment instantaneously (see Mangel et al 2006), and that re-
 cruitment tends asymptotically towards a finite value as B increases (Cushing 1988).
 58 The Beverton-Holt (B-H) relationship is typically used if recruitment is assumed to
 be limited primarily by food or habitat resources. Note that when βB is small, so
 60 that the exponential in Eq. (1) or the denominator in Eq. (2) are Taylor expanded, we
 obtain $S(B) = \alpha B(1 - \beta B)$, thus giving interpretation to the standard logistic model
 62 of population growth.

In open systems where resources are not locally limiting, Cushing (1973) devel-
 64 oped a power-law SRR

$$S(B) = \alpha B (\beta B)^{-1/n_c} = \alpha \beta^{-1/n_c} B^{\frac{n_c-1}{n_c}}. \quad (3)$$

Here, the third parameter n_c controls the rate of recruitment increase at high biomass densities, or the degree of compensation. In this case, if $n_c > 1$ recruitment continues to increase with increasing spawning biomass, but at a decreasing rate.

In an attempt to integrate the above relationships into a single function controlled by the degree of compensation, Shepherd (1982) observed that the behaviors exhibited by the Ricker, Cushing, and Beverton-Holt functions can be united into a single framework with three free parameters

$$S(B) = \frac{\alpha B}{1 + \beta B^{1/n}}, \text{ for } n > 0. \quad (4)$$

The parameters α and β again denote the initial rate of growth and the effects of density-dependence, respectively, while n is the degree of compensation. When $n < 1$, recruitment increases when B is low, and decreases when B is high, similar to the Ricker function. When $n = 1$, Eq. (4) simplifies to the Beverton-Holt (B-H) SRR, where recruitment saturates as B increases. For values of $n > 1$, recruitment behaves similarly to the Cushing function, maintaining a positive slope as B increases. The versatility of the Shepherd function comes at the cost of the additional degree of compensation parameter, which is often difficult to relate to observational data, and this has served to limit its adoption.

Using observational data, we are often unable to distinguish which model is most descriptive of the underlying dynamics. This has been a long-standing problem: in 1982, Gulland noted that “in many cases, the variability of the data makes it difficult to choose between alternative mathematical models” (pg. 17). Such variation may be a product of environmental variability, as well as differences in life-history. For instance, SRRs may be constrained by multiple, rather than a single compensatory event (Brooks and Powers 2007), and these species-specific characteristics can be controlled by many different aspects of fish reproductive biology (Morgan et al 2011).

In cases such as these, more complex models may be required, but this is at the cost of additional parameters, limiting the model's applicability to different systems.

Distinguishing between possible compensatory scenarios without assuming knowledge of the exact form the SRR would thus provide insight into the population dynamics of a fish species, without force-fitting a potentially incorrect recruitment model to observational data. Bayesian Nonparametric techniques provide one way to estimate descriptive characteristics of stock-recruitment functions based only on the data (Munch et al 2005).

Here we present an analytical approach to determine compensatory dynamics, without assuming knowledge of the specific SRR. We use a generalized modeling framework (*sensu* Gross and Feudel 2006; Gross et al 2009; Stiefs et al 2010; Yeakel et al 2011; Kuehn et al 2012) to derive relationships between the degree of compensation and the functional elasticities (the logarithmic derivative of a function, giving a measure of the change of the function relative to a change in its argument) of a continuous time generalized production model, as well as a discrete time age-structured model. Our results demonstrate that families of SRRs can be distinguished by these functional elasticities, which can be estimated from the dynamics of perturbations in fish biomass. We also show that some stock-recruitment families can be distinguished more easily than others, and that these differences are closely related to the stability of populations controlled by different compensatory dynamics.

2 Methods and Analysis

Despite the intrinsic simplifications introduced when using production or biomass dynamic models, they can offer direct insight into the mechanisms governing fish recruitment, and thus remain an important and oft-used tool in fisheries management (Mangel et al 2002; 2013), so we begin with them. We then extend our results and methods to a discrete time age-structured system, and show how functional elastic-

ities can distinguish between stock-recruitment families and provide direct insight
 116 into the stability regimes of populations with complex life histories.

2.1 Analysis of a Generalized Stock-Recruitment Model

118 In a generalized production model, we assume that biomass enlarges according to the
 function $S(B)$ and shrinks according to the function $D(B)$, such that biomass changes
 120 as

$$\frac{d}{dt}B = S(B) - D(B). \quad (5)$$

The enlargement function $S(B)$ may be assumed to have Ricker, B-H, or Cushing re-
 122 cruitment dynamics, whereas $D(B)$ is often assumed to be linear, such that $D(B) = zB$,
 where z is the rate of biomass loss due to fishing, natural mortality, or a combination
 124 thereof. However, in many cases we cannot assign a specific function to either $S(B)$
 or $D(B)$. Unfortunately, analysis of such a general model is not straightforward, since
 126 the steady state solution (B^* , where $S(B^*) = D(B^*)$) cannot be described analytically.
 In contrast, specific models present essentially the opposite problem: a steady state
 128 solution can often be computed, however the specific mathematical relationships may
 not accurately represent the dynamics of the population.

130 The general model presented in Eq. (5) cannot be solved at the steady state
 because the functions are unknown, however we can identify the unknown steady
 132 state(s) with the variable B^* . If we assume that $B^* > 0$ and that the signs of the
 growth and loss functions are biologically meaningful, then we can normalize the
 134 system to B^* . This allows us to define a set of normalized variables and functions.
 We set $S^* = S(B^*)$ and $D^* = D(B^*)$ and define

$$b = \frac{B}{B^*}, \quad s(b) = \frac{S(B)}{S^*}, \quad \text{and} \quad d(b) = \frac{D(B)}{D^*}. \quad (6)$$

136 This normalization procedure enables consideration of all positive steady states
 in the whole class of systems defined by Eq. (5), with the important property that
 138 at the steady state all generalized functions and variables are equal to unity ($b =$
 $1, s(1) = 1, d(1) = 1$) By substituting the normalized variables into Eq. (5), we obtain
 140 the normalized general production model

$$\frac{d}{dt}b = \frac{S^*}{B^*}s(b) - \frac{D^*}{B^*}d(b), \quad (7)$$

and under steady state conditions ($b = s(b) = d(b) = 1$), this simplifies to

$$0 = \frac{S^*}{B^*} - \frac{D^*}{B^*}. \quad (8)$$

142 Thus, at the steady state, the scaled growth and mortality coefficients are equivalent,
 allowing us to define the timescale of the system

$$\gamma = \frac{S^*}{B^*} = \frac{D^*}{B^*}. \quad (9)$$

144 This parameterization is useful because γ has a biologically relevant interpretation,
 and represents the biomass turnover rate. That is, for example, S^*/B^* has units of
 146 production per unit time of new biomass per unit of existing biomass. In general-
 ized modeling, coefficients such as γ are referred to as ‘scale parameters’ (Gross and
 148 Feudel 2006). Substituting γ into Eq. (7), the generalized equation is thus

$$\frac{d}{dt}b = \gamma(s(b) - d(b)). \quad (10)$$

Although the normalized functions $s(b)$ and $d(b)$ are still unknown, we can as-
 150 sess the dynamics of Eq. (10) by investigating the system under a small perturbation

evaluated at the steady state, accomplished by taking the derivative of the normalized
 152 system. The derivative of the right hand side of Eq. (10) is

$$\lambda|_* = \gamma \left(\left. \frac{\partial s(b)}{\partial b} \right|_* - \left. \frac{\partial d(b)}{\partial b} \right|_* \right) = \gamma(s_b - d_b), \quad (11)$$

where λ is the single eigenvalue of the system and $|_*$ indicates evaluation at the steady
 154 state B^* . The system is stable if $\lambda < 0$, and unstable if $\lambda > 0$. As λ moves upwards to-
 ward 0, the system approaches a saddle-node bifurcation (Guckenheimer and Holmes
 156 1983; Mangel 2006), a critical transition associated with the sudden appearance of a
 stable and unstable fixed point, changing the dynamics rapidly (Kuznetsov 1998).

158 The linearization of Eq. (10) reveals two additional parameters, s_b and d_b , which
 are the partial derivatives of the normalized functions $s(b)$ and $d(b)$, respectively.
 160 Partial derivatives of normalized functions are equivalent to the *elasticities* of the
 unnormalized functions (Gross and Feudel 2006; Yeakel et al 2011), which we show
 162 below. In general, elasticities provide a measure of the percent change of a function
 relative to the percent change in its argument

$$\begin{aligned} \text{Elasticity}\{F(a)\} &= \frac{a}{F(a)} \frac{\partial F(a)}{\partial a} \\ &= \lim_{x \rightarrow a} \frac{F(x) - F(a)}{x - a} \frac{a}{F(a)} = \lim_{x \rightarrow a} \frac{1 - \frac{F(x)}{F(a)}}{1 - \frac{x}{a}} \approx \frac{\% \Delta F(a)}{\% \Delta a}. \end{aligned} \quad (12)$$

164 Elasticities are commonly used in metabolic control theory (Fell 1992), economics
 (Sydsaeter and Hammond 1995) and life history theory (Horvitz et al 1997).

166 In generalized modeling, the elasticity of a function $F(X)$ with respect to its
 steady state X^* is alternatively written as the logarithmic derivative of the function

168 with respect to X^* (Yeakel et al 2011), and is equivalent to the partial derivative of
the normalized function $f(x)$,

$$f_x = \frac{X^*}{F^*} \frac{\partial F}{\partial X} \Big|_{x=1} = \frac{\partial \log F}{\partial \log X} \Big|_{x=1} = \frac{\partial f}{\partial x}. \quad (13)$$

170 Elasticities offer a number of advantages that are particularly useful for general-
ized modeling. First, an elasticity of a power-law function of the form $F(X) = aX^p$ is
172 equal to p . This can be shown by normalizing $F(X)$ to the equilibrium X^* , and taking
the derivative at the steady state, such that

$$f_x = \frac{\partial f}{\partial x} \Big|_* = \frac{\partial}{\partial x} \frac{aX^p}{aX^{*p}} \Big|_* = \frac{\partial}{\partial x} x^p \Big|_* = p.$$

174 For instance, if the function $D(B) = zB$ and z is a constant, then the elasticity is equal
to unity; if the function is quadratic, the elasticity is equal to 2; for constant functions,
176 the elasticity is equal to 0. For more complex functions, the value of the elasticity may
change with the value of the steady state (see below). Importantly, the elasticities of
178 functions governing the time-evolution of an animal population are representative
of the environmental conditions present during measurement. Thus elasticities are
180 not defined with respect to unmeasurable biological conditions that serve to bound
traditional functional relationships, such as half-maximum values or growth rates at
182 saturation (Fell and Sauro 1985; Fell 1992).

2.2 Relating functional elasticities to the degree of compensation

184 The degree of compensation in the Shepherd function (Eq. 4) is controlled by the
parameter n : if $n < 1$ the function is Ricker-like, if $n > 1$ the function is Cushing-like,
186 and if $n = 1$ it is equivalent to the B-H function (Shepherd 1982). In a generalized
modeling framework, the degree of compensation is related directly to the functional
188 elasticity. Given that B^* is large enough to experience density-dependent effects, if the

elasticity of growth $s_b < 0$ the population grows according to a Ricker-like function,
 190 if $s_b > 0$ the population grows according to a Cushing-like function, and if $s_b \rightarrow 0$ the
 population grows according to the B-H function. Thus, n and s_b are closely related,
 192 which can be shown by mapping the Shepherd function (Eq. 4) to the generalized
 model (Eq. 10), where

$$\begin{aligned} s(b) &= \frac{S(B)}{S(B^*)} = \frac{\alpha B}{1 + \beta B^{1/n}} \cdot \frac{1 + \beta B^{*1/n}}{\alpha B^*}, \\ &= \frac{1 + \beta B^{*1/n}}{1 + \beta B^{*1/n} b^{1/n}} b. \end{aligned}$$

194 The elasticity of growth is

$$s_b = 1 - \frac{\beta B^{*1/n}}{n(1 + \beta B^{*1/n})}. \quad (14)$$

Eq. (14) shows that the elasticity of growth depends on both the steady state biomass,
 196 as well as the degree of compensation, enabling direct comparisons between Ricker-
 like, Cushing-like, and B-H functions and their corresponding elasticities. For ex-
 198 ample, as B^* increases, if $n > 1$ (Cushing), then $s_b > 0$; if $n < 1$ (Ricker), then
 $s_b < 0$; if $n = 1$ (B-H), $s_b \rightarrow 0$ (Fig. 1). (This is more readily apparent if the quantity
 200 $(1/\beta B^{*1/n})(1/\beta B^{*1/n})^{-1}$ is factored into the rightmost term of Eq. 14.) Because the
 value of the elasticity holds for any function $S(B)$, this generalization is not isolated
 202 to the Shepherd equation, but extends to any function with degrees of compensation
 that can be categorized as ‘Ricker-like’, ‘Cushing-like’, or saturating. Thus, when
 204 density-dependent effects are present, if the value of the elasticity s_b can be deter-
 mined, a general functional family can be assigned to the observed recruitment dy-
 206 namics. This is a key relationship, because assignment of the functional family does
 not depend on the specific architecture of a given function.

208 If we assume that recruitment follows a Shepherd function, the degree of compensation can be determined directly if the elasticity s_b is

$$s_b = \frac{\gamma + \alpha(n-1)}{\alpha n}, \text{ or alternatively, } n = \frac{\gamma - \alpha}{\alpha(s_b - 1)}, \quad (15)$$

210 where as before, γ is the biomass turnover rate, and α is the recruitment rate at low biomass. From this relationship, we see that if $s_b < 1$, γ is constrained to vary between
 212 0 and α if n is to remain positive. Because γ is the biomass loss rate, it is evident that values greater than α (the maximum growth rate independent of density dependent
 214 effects) imply extinction of the population.

The discrimination of different governing functional forms (or families of functional forms) from observational data typically requires measures of statistical best fit using multiple years of stock-recruitment data (Munch et al 2005). Because these data are often highly variable and complicated by changes in birth and death rates over long timespans, distinguishing between functional forms can be problematic (Fig. 1a). However, because the elasticities of alternative functional families have non-overlapping ranges, they may be useful for determining the effects of density dependence on recruitment (Fig. 1b). Moreover, because the sign of the elasticity can differentiate between competing functional families, the determination of functional family from the elasticity of growth may be relatively error-tolerant.

The relationship between the elasticity of growth and the degree of compensation suggests that the Cushing SRR and Ricker SRR are qualitatively different than the B-H SRR. The reasoning for this is straightforward: the elasticity of growth is a continuous variable, and recruitment following the B-H function is defined by the elasticity $s_b = 1$, whereas Cushing-like and Ricker-like functions have elasticities that span a range of values. Mathematically, the elasticities of the Ricker- and Cushing-like functional families can be represented by non-overlapping intervals (Ricker: $s_b \in [-\infty, 0)$; Cushing: $s_b \in (0, \infty]$), whereas because the B-H function represents the boundary be-

tween the Ricker- and Cushing- functional families, it is a measure zero, or null set

234 (B-H: $s_b \in \emptyset$).

2.3 Measuring elasticities from time-series

236 We have shown that the degree of compensation can be calculated if the elasticity of
 growth is known. There exists a large body of literature in metabolic control theory
 238 for measuring elasticities in nature (which typically consist of experimental manip-
 ulations; Fell 1992), however these tools are not always appropriate for obtaining
 240 measurements from animal populations in the wild. We now show that the elasticity
 of growth can be measured from relatively small perturbations in fish biomass, and
 242 we provide a basic example using simulated data.

To begin, we consider single-species dynamics, where $dX/dt = F(X)$. We define
 244 deviation from the steady state, such that the population size at time t is some distance
 away from the equilibrium X^* as $\xi(t) = X(t) - X^*$. Then to first order

$$\frac{d}{dt}\xi(t) \approx F'(X^*)\xi. \quad (16)$$

246 For a single-species system, we observe that $F'(X^*)$ is also the single eigenvalue
 of the system, λ_f , and we use the subscript f to distinguish the eigenvalue in this
 248 example from the eigenvalue λ defined for the production model. Integrating Eq.
 (16), we find that $\xi(t) = \xi_0 e^{\lambda_f t}$ where ξ_0 is the initial deviation and $X(t) = X^* +$
 250 $\xi_0 e^{\lambda_f t}$. Thus, the eigenvalue of a single-species system is equivalent to the rate of
 relaxation to the steady state of the population trajectory after a small perturbation if
 252 $\lambda_f < 0$.

Our generalized analysis of Eq. (5) shows that $\lambda = \gamma(s_b - d_b)$. For now, we will
 254 assume that λ can be measured. To determine which of the three functional families
 depicted in Fig. (1a) drive recruitment dynamics, we must determine the elasticity
 256 of growth, where $s_b = \lambda/\gamma + d_b$. If mortality is assumed to be governed by a linear

function, such that $d_b = 1$, then the criteria are simply defined by comparing the
 258 magnitude of the relaxation rate, λ , to the timescale of the system, γ (Table 1). If
 we assume that the steady state is stable ($\lambda < 0$), recruitment is driven by a Ricker-
 260 like function if $\lambda < -\gamma$, recruitment is driven by the B-H function if $\lambda = -\gamma$, and
 recruitment is driven by a Cushing-like function if $\lambda > -\gamma$ (Fig. 1a). Because we do
 262 not presume to know the exact architecture of the stock-recruitment function, these
 relationships are predictive of general families of models. If we assume that growth
 264 is governed by the Shepherd function, the general relationship between the degree of
 compensation and the relaxation rate is (cf. Eqn 15)

$$n = \gamma \frac{\gamma - \alpha}{\alpha(\lambda + \gamma d_b - \gamma)}. \quad (17)$$

266 which can be simplified further assuming that mortality is governed by a linear func-
 tion, such that

$$n = \gamma \frac{\gamma - \alpha}{\alpha \lambda}. \quad (18)$$

268 As the system approaches the saddle-node bifurcation at $\lambda = 0$, small errors in
 λ are likely to generate large errors in the degree of compensation (Eq. 18, Fig. 2),
 270 such that Ricker-like SRRs result in measurements that are more error-tolerant than
 Cushing-like SRRs. Moreover, because an elasticity of growth $s_b < 1$ produces dy-
 272 namics with a single non-trivial stable steady state (assuming the elasticity of mor-
 tality $d_b = 1$), only Cushing-like SRRs can come close to the saddle-node bifurcation
 274 at $\lambda = 0$. The rate at which the saddle-node bifurcation is reached as n increases is
 contingent on the biomass turnover rate γ , where turnover rates intermediate to 0 and
 276 α approach the bifurcation more slowly. If the turnover rate is greater than α , $\lambda > 0$
 and the system becomes unstable.

278 2.4 Estimating the degree of compensation from fluctuations in fish biomass

We have derived a relationship between the degree of compensation n and the elastic-
 280 ity of growth s_b , and have shown how - in principle - elasticities could be measured
 from short-term fluctuations in time-series data. To elaborate this idea, we constructed
 282 a stochastic model with growth following the Shepherd function and mortality due to
 both natural causes M and fishing F , coupled with observation error. We perturbed
 284 the system at time $t = t_i$ by eliminating the fishing mortality term (the end of a fish-
 ing period) until a steady state was reached at the terminal time $t = T$. We included
 286 normally distributed observation error \tilde{P} with mean zero and standard deviation σ .
 Accordingly, observations of fish biomass $B_{\text{obs}}(t)$ change are then

$$\frac{d}{dt}B = \frac{\alpha B}{1 + \beta B^{1/n}} - (M + \delta F)B,$$

$$B_{\text{obs}}(t) = B(t) + \sigma \tilde{P},$$

288 where δ controls fishing mortality. During the fishing time interval $t_0 \leq t < t_i$, $\delta = 1$;
 during the non-fishing time interval $t_i \leq t < T$, $\delta = 0$ (e.g. Fig. 3).

290 Given the Gaussian assumption about the observation error, we assume that the
 system trajectory behaves as $B_{\text{obs}}(t) \sim N\{c(1 - e^{-\lambda t}), \sigma\}$ close to the steady state.
 292 The stochastic trajectory thus depends on the unknown variables c , λ , and σ , which
 we determine using a likelihood approach where k is the number of observations from
 294 the end of the fishing period until the trajectory reaches its steady state in the absence

of fishing at $t = T$. This problem can be simplified, as the variables c and σ can be
 296 written in terms of λ to obtain the log-likelihood (Hilborn and Mangel 1997)

$$\log \mathcal{L}(\lambda) = -\frac{k}{2} \log(2\pi) - \frac{k}{2} \log \left\{ \frac{1}{k} \left(\sum_{t=t_i}^T B(t) - \frac{\sum_{t=t_i}^T B(t)(1 - e^{-\lambda t})}{\sum_{t=t_i}^T (1 - e^{-\lambda t})} \right)^2 \right\} - \frac{k}{2},$$
(19)

which we use to find the maximum likelihood estimate for the eigenvalue λ_{MLE} .

308 We aim to discriminate between different families of functional forms using the
 maximum likelihood estimate for the rate at which a population trajectory returns
 300 to its steady state after a perturbation. If the rate of relaxation is known, the degree
 of compensation can be calculated from Eq. (18). To determine the accuracy of our
 302 model estimates across different degrees of observation noise, we calculated λ_{MLE}
 as a function of the coefficient of variation ($\text{CV} = \sigma/B^*$) for three compensation
 304 scenarios: Ricker ($n = 0.5$), Cushing ($n = 1.5$), and B-H ($n = 1$). After estimating
 λ_{MLE} , we calculated the degree of compensation, n_{MLE} from Eq. (18), and determined
 306 the probability that n was correctly distinguished with respect to alternative stock-
 recruitment functions (Fig. 4a,b), as well as the probability that the functional family
 308 was correctly identified (Fig. 4a,c).

3 Results

310 The analytical relationship between the degree of compensation n and the elasticity
 of growth s_b (Eq. 18) suggests that populations growing in accordance to Ricker-like
 312 functions should be less difficult to measure accurately than those growing in ac-
 cordance to Cushing-like functions (Fig. 2a). In general, our simulation experiment
 314 showed that the rate of relaxation can be estimated from moderately noisy data, and
 that there were large differences in the measurement accuracy for different functional
 316 families. The estimated rate of relaxation λ_{MLE} , and by transformation n_{MLE} , is esti-

318 mated more accurately for Ricker-like and B-H functions than for Cushing-like func-
tions (Fig. 4a). We note that the mean value of our estimates always diverged from
the set value of n because the rate of return equation is only accurate at values very
320 close to B^* and is therefore a necessarily crude estimate of the solution to $B_{\text{obs}}(t)$.

Despite differences in measurement accuracy, the probability that the correct
322 stock-recruitment function was distinguishable from the other SRRs declined approx-
imately linearly for both Ricker and Cushing models after $CV = 0.15$, while that for
324 the B-H model declined nonlinearly (Fig. 4b). The B-H model was more difficult to
distinguish because estimates of n overlapped values for both neighboring models.
326 However, this comparison is somewhat arbitrary, and the more important question re-
lates to the probability that the functional family is correctly determined with respect
328 to other potential families of functions. Our results showed that the probably of cor-
rectly determining the functional family from λ_{MLE} remained relatively high as CV
330 increased (Fig. 4c) for both Ricker-like and Cushing-like functions. The probably that
Ricker-like functions were correctly distinguished was generally greater than 0.6 for
332 $CV \leq 0.30$. The same probability was greater than 0.8 for $CV \leq 0.5$ for Cushing-like
functions, due primarily to the greater range of n for the Cushing functional form.
334 Because the B-H function is boundary between functional families (see Methods),
the probability that it was correctly distinguished was always 0.

336 **4 An Example With Age Structure**

Production models effectively summarize the recruitment dynamics of fish popula-
338 tions, and in some cases can provide robust measures of fisheries reference points
(MacCall 2002; Mangel et al 2010; 2013). However, the influence of age-related dif-
340 ferences in growth and mortality can have large effects on the dynamics of fish popu-
lations (Mangel et al 2006; Shelton and Mangel 2011). In this section we build upon
342 our prior results and expand the generalized modeling schema to discrete time, age-

structured models. The extension of generalized modeling to discrete time systems is
 344 useful in its own right, as it provides a method for the dynamical analysis of whole
 classes of discrete time models (*sensu* Gross and Feudel 2006). First, we briefly illus-
 346 trate an extension of the generalized modeling approach to an age-structured discrete
 time system. Second, we show how the degree of compensation in an age-structured
 348 system is related to the elasticities of growth and finish by showing how measure-
 ments of elasticities in the age-structured model provide important insight into system
 350 stability.

We consider an age-structured model where the number of recruits $X(t + 1)$ is
 352 governed by spawning stock biomass, $B_s(t)$, depending on the degree of compensa-
 tion n . The number of individuals in the mature age class Y is the sum of returning
 354 adults and incoming recruits, where adult mortality is given by M_y and recruit mortal-
 ity is given by M_x . It follows that spawning stock biomass is calculated by the number
 356 of mature individuals times the average mass of individuals W_y . The age-structured
 model is thus

$$\begin{aligned}
 X(t + 1) &= F(B_s, t) &&= \frac{\alpha B_s(t)}{1 + \beta B_s(t)^{1/n}}, \\
 Y(t + 1) &= G(X, t) + H(Y, t) &&= X(t)e^{-M_x} + Y(t)e^{-M_y}, \\
 B_s(t + 1) &= K(Y, t) &&= Y(t)W_y.
 \end{aligned} \tag{20}$$

358 We can determine the steady state condition X^* (where $X(t + 1) = X(t)$) in terms of
 spawning stock biomass B_s^* because at the steady state $B_s^* = Y^*W_y$, such that

$$B_s^* = X^* \frac{e^{-M_x} W_y}{1 - e^{-M_y}} = X^* W_f^*. \tag{21}$$

360 The primary difference between the age-structured and production models is that
 mortality is not assumed to occur simultaneously with recruitment, and this yields

362 dynamics that diverge strongly from those predicted by the production model. We
 note that this 3-dimensional model can be slightly modified and collapsed such that
 364 $B_s(t) = Y(t)W_y$, and this has little effect on the qualitative dynamics.

The normalization of the age-structured system is analogous to the normaliza-
 366 tion of the production model (Eq. 7), however because the age-structured system
 is composed of difference rather than differential equations, the steady state condi-
 368 tion requires that the scale parameters are defined differently than before. For ex-
 ample, $y(t+1) = (G^*/Y^*)g(x,t) + (H^*/Y^*)h(y,t)$ is defined at the steady state $1 =$
 370 $G^*/Y^* + H^*/Y^*$, such that we define the ratio of incoming recruits to the abundance
 of the mature age-class $\gamma_y = G^*/Y^*$ and the ratio of returning adults to the abundance
 372 of the mature age-class $(1 - \gamma_y) = H^*/Y^*$. These coefficients are thus the propor-
 tional contributions of recruit and mature age-classes to spawning stock biomass at
 374 the steady state. The generalized system is then

$$\begin{aligned} x(t+1) &= \gamma_x f(b,t), \\ y(t+1) &= \gamma_y g(x,t) + (1 - \gamma_y)h(y,t), \\ b(t+1) &= \gamma_b k(y,t). \end{aligned} \tag{22}$$

We can immediately simplify the problem by observing that the scale parameters for
 376 recruits and biomass can be reduced to

$$\begin{aligned} \gamma_x &= \frac{F^*}{X^*} = \frac{\alpha W_f^*}{1 + \beta (W_f^* X^*)^{1/n}} = 1, \\ \gamma_b &= \frac{K^*}{B_s^*} = 1. \end{aligned} \tag{23}$$

For the production model, elasticities were defined with respect to the linearized
 378 system (Eq. 11). Because the age-structured system is multi-dimensional, the lin-

linearization is defined by the Jacobian matrix evaluated at the steady state $\mathbf{J}|_*$, where
 380 each element is defined by the partial derivative of each differential equation with
 respect to each variable. The elasticities of the generalized system can then be calcu-
 382 lated, such that

$$\mathbf{J}|_* = \begin{pmatrix} \left. \frac{\partial F}{\partial X} \right|_* & \left. \frac{\partial F}{\partial Y} \right|_* & \left. \frac{\partial F}{\partial B_s} \right|_* \\ \left. \frac{\partial G+H}{\partial X} \right|_* & \left. \frac{\partial G+H}{\partial Y} \right|_* & \left. \frac{\partial G+H}{\partial B_s} \right|_* \\ \left. \frac{\partial K}{\partial X} \right|_* & \left. \frac{\partial K}{\partial Y} \right|_* & \left. \frac{\partial K}{\partial B_s} \right|_* \end{pmatrix} = \begin{pmatrix} 0 & 0 & f_b \\ \gamma_y (1 - \gamma_y) & 0 & 0 \\ 0 & 1 & 0 \end{pmatrix}, \quad (24)$$

and for the specific age-structured model, $\gamma_y = 1 - e^{-M_y}$, and

$$f_b = \frac{\alpha W_f^* (n-1) + 1}{\alpha W_f^* n}. \quad (25)$$

384 The Jacobian matrix determines the stability of the system; we solve for the eigenval-
 ues that satisfy the characteristic equation $\text{Det}(\mathbf{J}|_* - \lambda \mathbf{I}) = 0$, where \mathbf{I} is the identity
 386 matrix. From Eq. (24), the characteristic equation is $f_b \gamma_y + \lambda^2 - \gamma_y \lambda^2 - \lambda^3 = 0$, which
 yields three distinct eigenvalues, and though the solutions for these eigenvalues are
 388 large and unwieldy, they can be easily derived with algebraic computing languages
 such as Maple or Mathematica.

390 Simulation of the age-structured system (where $\alpha = 8$, $\beta = 1/80$, $M_x = 0.2$, $M_y =$
 0.7 , and $W_y = 2$) across a range of values for the degree of compensation reveals a
 392 single steady state for $n > 0.376$. For $n < 0.376$, stable cycles emerge, which in turn
 give rise to five-period cycles for lower values of n (Fig. 5a,b). In discrete time sys-
 394 tems, the emergence of cyclic conditions can result from crossing a Neimark-Sacker
 bifurcation (cf. Guill et al 2011a;b), which occurs when a pair of complex conju-
 396 gate eigenvalues cross the unit circle on the complex plane. If λ_1 and λ_2 are the
 complex conjugate eigenvalue pair, the test-function for this condition is $\lambda_1 \lambda_2 = 1$
 398 (Kuznetsov 1998). Using solutions for λ_1 and λ_2 from the characteristic equation, we
 numerically determined that a supercritical Neimark-Sacker bifurcation is crossed at

400 $n = 0.376$ (Fig. 5a,c). Supercritical Neimark-Sacker bifurcations yield stable closed
 invariant curves, such that local trajectories initiated interior and exterior to the cycle
 402 are attracted to the curve (cf. Fig. 5b; Kuznetsov 1998). Predictions of population
 dynamics are thus possible, but only if the degree of compensation, in addition to the
 404 other parameters, is known. As before, the specific age-structured model introduces
 strong assumptions regarding functional forms, and these assumptions may not hold
 406 (or be conducive to measurement) in many situations.

Because the degree of compensation is related directly to the elasticity of growth
 408 (Eq. 25), we can use the generalized age-structured system to gather direct insight into
 the potential dynamics applicable to any class of models substituted into the general
 410 functions $F(B)$, $G(X)$, $H(Y)$, and $K(Y)$. Although the test-function for the Neimark-
 Sacker bifurcation is not analytically tractable (even for the generalized system), we
 412 can numerically simulate the relationship between the elasticity of growth f_b , the
 proportion of maturing recruits to the mature age class γ_y (which has a value of 0.50
 414 in the simulated age-structured model), and the test-function $\lambda_1 \lambda_2$. Our numerical re-
 sults show that only Ricker-like SRRs can result in cyclic dynamics ($\lambda_1 \lambda_2 \geq 1$; Fig.
 416 5d). Moreover, we observe that cyclic dynamics can only emerge if $f_b \leq -1$ for any
 potential value of γ_y , and this result applies to all potential SRRs. Accordingly, as
 418 the ratio of maturing recruits declines (low γ_y ; realized as the mortality of the mature
 age-class M_y decreases), cyclic dynamics are less likely to occur unless the elastic-
 420 ity of growth is extremely low, which is biologically unreasonable. As the ratio of
 maturing recruits increases (higher mature age-class mortality), the opposite occurs,
 422 and cyclic dynamics are more likely for a broader range of Ricker-like SRRs. We
 have thus obtained a very powerful result: independent of the particular functions
 424 introduced into the general age-structured system, cyclic dynamics require 1) that
 spawning stock biomass includes a relatively large proportion of incoming recruits,
 426 and 2) that compensatory dynamics are driven by a Ricker-like function, where the
 elasticity of growth has a value ≤ -1 .

428 The relationship between recruitment, the elasticity of growth, and cyclic dy-
namics has predictive power, in particular because it is general without assumptions
430 regarding the exact shapes of functional responses. For example, pink salmon (*On-*
corhynchus gorbuscha) are a widespread species with complex population dynamics
432 (Radchenko et al 2007). Depensatory dynamics are responsible for a large source of
embryo mortality as spawning individuals compete for viable nests, such that Ricker-
434 like models are generally predictive of stock recruitment relationships (May 1974;
Myers et al 1995). Moreover, pink salmon are semelparous, such that there is no
436 overlap in spawning stock biomass between generations. In our generalized mod-
eling framework, this corresponds to an elasticity of growth $f_b < 0$, and complete
438 turnover of the adult age-class, such that γ_y is close to unity. From Fig. 5d, we ob-
serve that cyclic dynamics are inevitable if $f_b < -1$ as $\gamma_y \rightarrow 1$. In nature, pink salmon
440 populations are strongly cyclic, generally on the order of two-year cycles, and this is
thought to be caused by density-dependent mortality reinforced by external sources
442 of stochasticity (Krkosek et al 2011). Thus, we observe that by relating the elasticity
of growth to stability regimes, knowledge of general aspects of population dynamics
444 - without assuming specific functional relationships - can provide direct insights into
the compensatory dynamics of age-structured populations.

446 5 Discussion

We have shown that the elasticity of growth in a generalized production model can be
448 related directly to the degree of compensation parameter that determines Ricker-like,
Cushing-like, or Beverton-Holt behaviors. The elasticity of growth is useful because
450 it is defined with respect to the biological and environmental conditions present dur-
ing measurement, and thus can be estimated from limited time-series data. Moreover,
452 because large ranges of the elasticity of growth, and by extension the rate of re-
laxation, characterize families of functional forms, these measures are error tolerant

454 (Fig 4c), particularly if the goal is to distinguish between SRRs with Ricker-like or
Cushing-like recruitment dynamics.

456 The functional elasticities of both production and age-structured models can be
used to determine directly the compensatory dynamics driving SRRs. This method
458 may be of most use to recent fisheries, where long-term time-series data do not yet
exist. Because we have employed elasticities in a generalized modeling framework,
460 they are well-suited to inform knowledge of the general nature of compensation, and
thus may be particularly useful for developing priors for parameters in flexible SRRs,
462 such as the degree of compensation in the Shepherd model. Determining SRRs from
elasticities may also be useful if populations have highly variable recruitment dynam-
464 ics, or dynamics that are strongly sensitive to changing environmental conditions,
and it may be instructive to consider alternative approaches for measuring elasticities
466 across a broader range of management scenarios.

Acknowledgements We thank S. Allesina, M.P. Beakes D. Braun, T. Gross, C. Kuehn, T. Levi, A. Mac-
468 Call, J.W. Moore, S. Munch, M. Novak, C.C. Phillis and A.O. Shelton for many helpful discussions and
comments. We also thank the Dynamics of Biological Networks Lab at the Max-Planck Institute for the
470 Physics of Complex Systems and the University of Bristol, for sharing the ideas and knowledge that in-
spired this work. This project was partially funded by the Center for Stock Assessment and Research, a
472 partnership between the Fisheries Ecology Division, NOAA Fisheries, Santa Cruz, CA and the University
of California, Santa Cruz and by NSF grant EF- 0924195 to M.M.

474 **References**

- 476 Beverton RJH, Holt SJ (1957) On the dynamics of exploited fish populations. *Fish and Fisheries*, Vol. 11, Springer, New York
- 478 Brooks EN, Powers JE (2007) Generalized compensation in stock-recruit functions: properties and implications for management. *ICES J Mar Sci* 64(3):413–424
- 480 Cushing DH (1973) The dependence of recruitment on parent stock. *J Fish Res Bd Can* 30:1965–1976
- 482 Cushing DH (1988) The problems of stock and recruitment. In: *Fish population dynamics: the implications for management*, John Wiley & Sons Inc
- 484 Fell DA (1992) Metabolic control analysis: a survey of its theoretical and experimental development. *Biochem J* 286:313–330
- 486 Fell DA, Sauro HM (1985) Metabolic control and its analysis. *Eur J Biochem* 148(3):555–561
- 488 Gross T, Feudel U (2006) Generalized models as a universal approach to the analysis of nonlinear dynamical systems. *Phys Rev E* 73(1 Pt 2):016205
- 490 Gross T, Rudolf L, Levin SA, Dieckmann U (2009) Generalized models reveal stabilizing factors in food webs. *Science* 325(5941):747–750
- 492 Guckenheimer J, Holmes P (1983) *Nonlinear oscillations, dynamical systems, and bifurcations of vector fields*. Springer, Berlin, Heidelberg, New York
- 494 Guill C, Drossel B, Just W, Carmack E (2011a) A three-species model explaining cyclic dominance of Pacific salmon. *J Theor Biol* 276(1):16–21
- 496 Guill C, Reichardt B, Drossel B, Just W (2011b) Coexisting patterns of population oscillations: the degenerate Neimark-Sacker bifurcation as a generic mechanism. *Phys Rev E* 83(2):021910
- 498 Gulland JA (1988) The analysis of data and development of models. In: *Fish population dynamics: the implications for management*, John Wiley & Sons Inc

- 500 Hilborn R, Mangel M (1997) *The ecological detective: Confronting models with data.*
Princeton University Press, Princeton
- 502 Horvitz C, Schemske DW, Caswell H (1997) The relative “importance” of life-history
stages to population growth: prospective and retrospective analyses. In: *Structured-*
504 *population models in marine, terrestrial, and freshwater systems*, Chapman and
Hall, New York, pp 247–271
- 506 Krkosek M, Hilborn R, Peterman RM, Quinn TP (2011) Cycles, stochasticity
and density dependence in pink salmon population dynamics. *Proc Roy Soc B*
508 278(1714):2060–2068
- Kuehn C, Siegmund S, Gross T (2012) Dynamical analysis of evolution equations in
510 generalized models. *IMA J Appl Math*
- Kuznetsov Y (1998) *Elements of applied bifurcation theory.* Springer New York
- 512 MacCall AD (2002) Use of known-biomass production models to determine produc-
tivity of west coast groundfish stocks. *N Am J Fish Manage* 22(1):272–279
- 514 Mangel M (2006) *The theoretical biologist’s toolbox: Quantitative methods for ecol-
ogy and evolutionary biology.* Cambridge University Press, Cambridge
- 516 Mangel M, Marinovic B, Pomeroy C, Croll D (2002) Requiem for Ricker: Unpacking
MSY. *B Mar Sci* 70(2):763–781
- 518 Mangel M, Levin P, Patil A (2006) Using life history and persistence criteria to pri-
oritize habitats for management and conservation. *Ecol Appl* 16(2):797–806
- 520 Mangel M, Brodziak J, DiNardo G (2010) Reproductive ecology and scientific in-
ference of steepness: a fundamental metric of population dynamics and strategic
522 fisheries management. *Fish Fish* 11:89–104
- Mangel M, MacCall AD, Brodziak JK, Dick EJ, Forrest RE, Pourzand R, Ralston S
524 (2013) A perspective on steepness, reference points, and stock assessment. *Can J
Fish Aquat Sci* pp 1–64
- 526 May RM (1974) Biological populations with nonoverlapping generations: Stable
points, stable cycles, and chaos. *Science* 186(4164):645–647

- 528 Morgan MJ, Perez-Rodriguez A, Saborido-Rey F, Marshall CT (2011) Does in-
creased information about reproductive potential result in better prediction of re-
530 cruitment? *Can J Fish Aquat Sci* 68(8):1361–1368
- Munch SB, Kottas A, Mangel M (2005) Bayesian nonparametric analysis of stock-
532 recruitment relationships. *Can J Fish Aquat Sci* 62(8):1808–1821
- Myers RA, Barrowman NJ, Hutchings JA, Rosenberg AA (1995) Population dynam-
534 ics of exploited fish stocks at low population levels. *Science* 269(5227):1106–1108
- Radchenko VI, Temnykh OS, Lapko VV (2007) Trends in abundance and biologi-
536 cal characteristics of pink salmon (*Oncorhynchus gorbuscha*) in the North Pacific
Ocean. *North Pac Anadromous Fish Comm Bull* 4:7–21
- 538 Ricker W (1954) Stock and recruitment. *Can J Fish Aquat Sci* 11(5):559–623
- Shelton AO, Mangel M (2011) Fluctuations of fish populations and the magnifying
540 effects of fishing. *Proc Natl Acad Sci USA* 108(17):7075–7080
- Shepherd J (1982) A versatile new stock-recruitment relationship for fisheries, and
542 the construction of sustainable yield curves. *J Conseil* 40(1):67–75
- Sissenwine MP, Shepherd JG (1987) An alternative perspective on recruitment over-
544 fishing and biological reference points. *Can J Fish Aquat Sci* 44(4):913–918
- Stiefs D, van Voorn GAK, Kooi BW, Feudel U, Gross T (2010) Food quality in
546 producer-grazer models: A generalized analysis. *Am Nat* 176(3):367–380
- Sydsaeter K, Hammond PJ (1995) *Essential Mathematics for Economic Analysis*.
548 Prentice-Hall Inc., New Jersey
- Yeakel JD, Stiefs D, Novak M, Gross T (2011) Generalized modeling of ecological
550 population dynamics. *Theor Ecol* 4(2):179–194

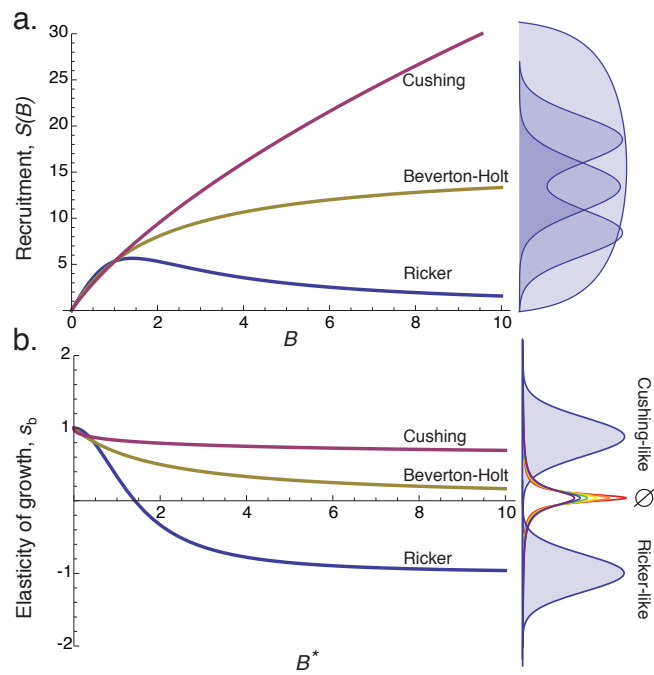


Fig. 1 a. Recruitment $S(B)$ as a function of spawning stock biomass B . b. The elasticity of growth s_b as a function of the steady state spawning stock biomass B^* . The distributions to the right represent potential measurements of recruitment (a.) and the elasticity of growth (b.) for Ricker, B-H, and Cushing recruitment functions. Although measurements for SRRs overlap in (a.), the elasticities of the Ricker- and Cushing-like functional families can be represented by non-overlapping intervals. Ricker: $s_b \in [-\infty, 0)$; Cushing: $s_b \in (0, \infty]$, whereas the B-H function is the boundary between Ricker- and Cushing- functional families, such that $s_b \in \emptyset$.

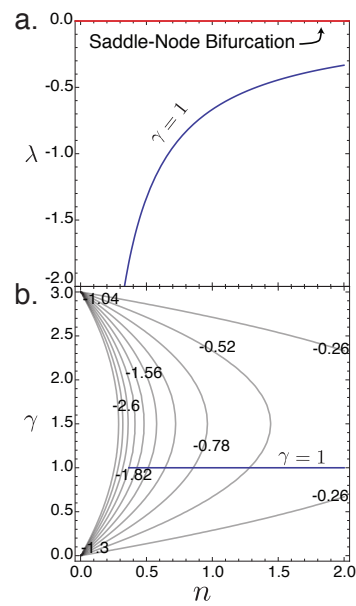


Fig. 2 a. The rate of relaxation to the steady state λ vs. the degree of compensation n for a biomass turnover rate $\gamma = 1$. The red line at $\lambda = 0$ denotes a saddle-node bifurcation below which the system is stable, and above which the system is unstable. b. The biomass turnover rate γ as a function of the degree of compensation n and the rate of relaxation λ (contour lines). The trajectory shown in (A.) is denoted by the blue line. Values of $0 < \gamma < (\alpha = 3)$ result in stable dynamics, and only Cushing-like functions, where $n > 1$ can result in values of λ close to the saddle-node bifurcation.

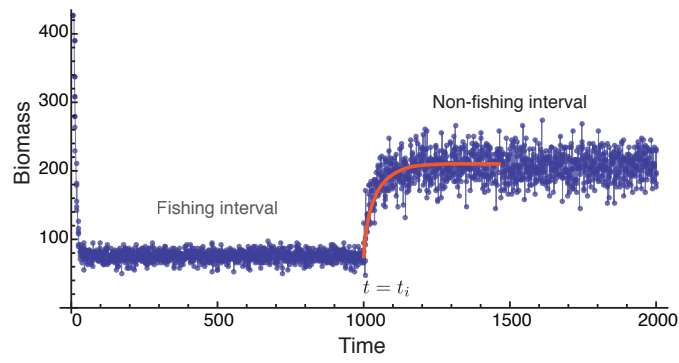


Fig. 3 An example of the transition from a fishing to a non-fishing interval used to measure the rate of relaxation λ from time-series data. The non-fishing interval is initiated at $t = t_i$, and biomass values immediately after t_i can be used to find the maximum likelihood estimate for λ . The best-fit trajectory using the likelihood technique is shown in orange.

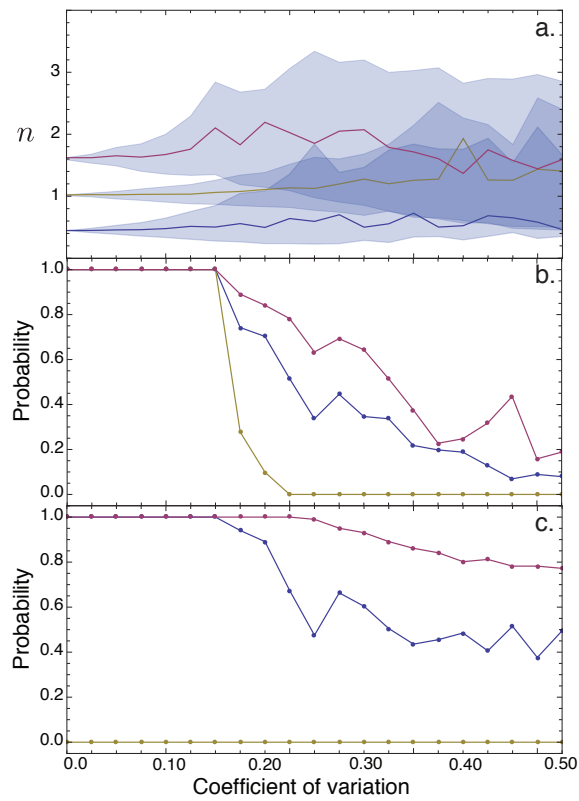


Fig. 4 a. Estimation of the degree of compensation as a function of the coefficient of variation for 6300 simulated population trajectories (300 for each of 21 different values of CV). Shaded areas show the standard deviation of estimated n values, while colored lines show the means (blue: Ricker; red: Cushing; yellow: B-H). b. The probability of correctly identifying the specific model from the others (Ricker: $n = 0.5$; Cushing: $n = 1.5$, and B-H: $n = 1$). c. The probability of correctly identifying the SRR family (Ricker: $n < 1$; Cushing: $n > 1$; B-H: $n = 1$). The probability of measuring the B-H SRR is always zero.

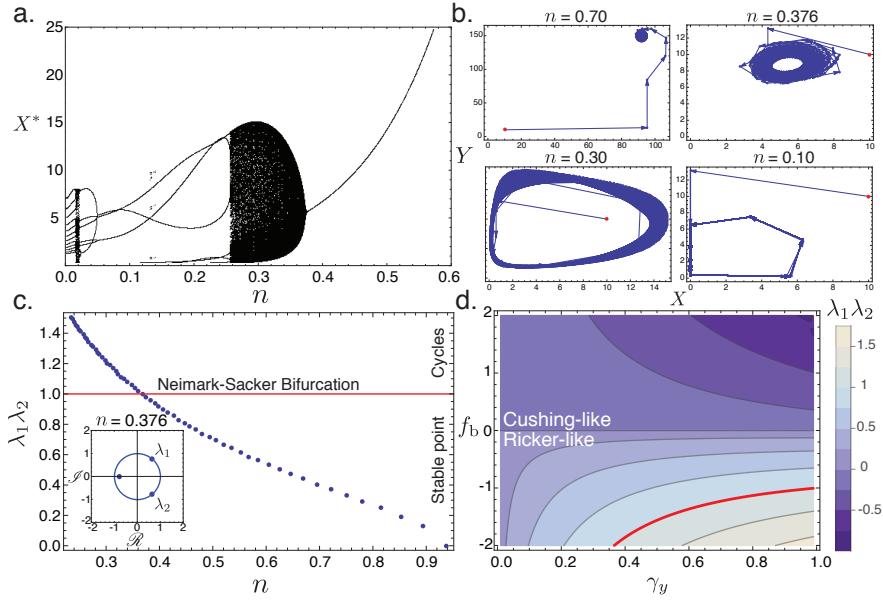


Fig. 5 a. Bifurcation diagram showing the onset of cycles followed by multi-period oscillations for the age-structured model as the degree of compensation lowers beyond $n = 0.376$. b. Examples of the corresponding dynamics where $n = 0.70$, $n = 0.376$, $n = 0.30$, and $n = 0.10$. c. Values of the test-function $\lambda_1 \lambda_2$ across different values of n for the specific model. A Neimark-Sacker bifurcation exists at $\lambda_1 \lambda_2 = 1$, which is crossed at $n = 0.376$. This condition exists when two complex conjugate eigenvalues cross the unit circle on the complex plane (inset). d. Numerically estimated values for the test-function $\lambda_1 \lambda_2$, given the elasticity of growth f_b and the ratio of incoming recruits to the mature age-class γ_y . The red contour denotes the Neimark-Sacker bifurcation condition; systems below this contour have cyclic dynamics.

Table 1 Criteria for determining the elasticity of growth s_b from the rate of return to the steady state after a perturbation, λ , for the production model. The non-overlapping intervals for the elasticity of growth uniquely identify of Ricker-like, Beverton-Holt, and Cushing-like recruitment dynamics.

Model	Elasticity ($B^* \gg 0$)	Criterion
Ricker-like	$s_b < 0$ s.t. $\frac{\lambda}{\gamma} + d_b < 0$	$\lambda < -\gamma d_b$
Beverton-Holt	$s_b = 0$ s.t. $\frac{\lambda}{\gamma} + d_b = 0$	$\lambda = -\gamma d_b$
Cushing-like	$s_b > 0$ s.t. $\frac{\lambda}{\gamma} + d_b > 0$	$\lambda > -\gamma d_b$